Full-sky searches for anisotropies in UHECR arrival directions with the Pierre Auger Observatory and the Telescope Array

A. di Matteo[1], T. Bister, J. Biteau, L. Caccianiga, O. Deligny, T. Fujii, D. Harari, D. Ivanov, K. Kawata, J.P. Lundquist, R. Menezes, D. Mockler, T. Nonaka, H. Sagawa, P. Tinyakov, I. Tkachev, and S. Troitsky, for the Pierre Auger[2] and Telescope Array[3] collaborations

[1]Istituto Nazionale di Fisica Nucleare (INFN), Sezione di Torino, Turin, Italy <armando.dimatteo@to.infn.it>
[2]Full author list: http://www.auger.org/archive/authors_icrc_2019.html <auger_spokespersons@fnal.gov>
[3]Full author list: http://www.telescopearray.org/research/collaborators <ta-icrc@cosmic.utah.edu>

36th International Cosmic Ray Conference (ICRC 2019)
24 July – 1 August 2019, Madison, Wisconsin, USA

Outline

1. Introduction
   - Motivation and recent results
   - Datasets used in this work
2. Results
   - Search for full-sky large-scale anisotropies at relatively low energies
   - Blind search for medium-scale anisotropies at the highest energies
   - Search for excesses along the supergalactic plane or the Local sheet
3. Possible future analyses

The detectors

Telescope Array experiment

- Located at 39.3° N, 112.9° W, 1400 m a.s.l. (Millard County, Utah, USA)
- Main array: 507 plastic scintillator detectors in a 1.2 km square grid (700 km^2 total)
- Taking data since May 2008

147 collaborators
36 institutions
6 countries

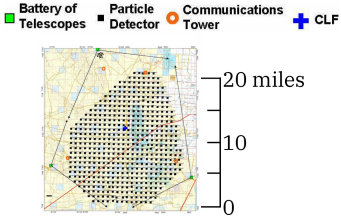

Pierre Auger Observatory

- Located at 35.2° S, 69.2° W, 1400 m a.s.l. (Mendoza Province, Argentina)
- Main array: 1600 water Cherenkov detectors in a 1.5 km triangular grid (3000 km^2 total)
- Taking data since January 2004

385 collaborators
89 institutions
17 countries

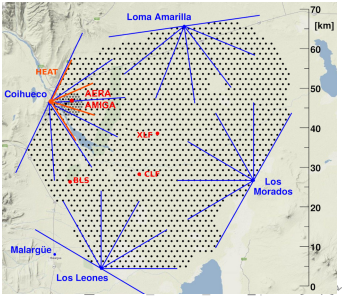

Motivation

- UHECRs interact with background photons → propagation lengths limited to tens of Mpc
- The Universe is not homogeneous on these scales → we should see the source distribution.
  - OTOH, magnetic deflections $\sim 30^\circ \left(\frac{E/Z}{10\ \mathrm{EeV}}\right)^{-1}$ can blur and distort the picture.
- See e.g. AdM and P. Tinyakov (2018) for predictions.

Pisces–Cetus Supercluster Complex

- Pisces–Cetus Supercluster
- various chains
- Laniakea Supercluster:
  - Hydra–Centaurus Supercluster
  - Pavo–Indus Supercluster
  - Southern Supercluster
  - Virgo Supercluster:
    - Virgo Cluster
    - Local Sheet (**you are here**)

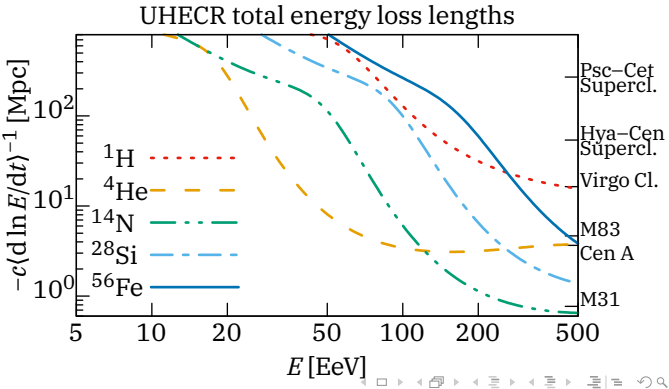

Recently published results

Relatively low energies

$1\ \text{EeV} \leq E < 3.2\ \text{EeV}$: **isotropic** flux → fraction of Galactic protons $\lesssim 10\%$ / $\leq 1.3\%$ at 95% C.L. (Auger 2013, TA 2017)

$E \geq 4\ \text{EeV}$: **dipole** moment $(5.5 \pm 0.8)\% \times \left(\frac{E}{10\ \text{EeV}}\right)^{0.8\pm0.2}$; no statistically significant quadrupole (Auger 2018)

The highest energies

$E \geq 39\ \text{EeV}$: indication of correlation with positions and fluxes of nearby **starburst galaxies** $(13^{+4}_{-3})^\circ$ smearing, plus $(90 \pm 4)\%$ isotropic background (Auger 2018) (TA 2018: not enough data to confirm or refute)

$16\ \text{EeV} \leq E < 56\ \text{EeV}$ and $E \geq 56\ \text{EeV}$: indication of a **coldspot** and a **hotspot** (respectively) 28°-radius around $(9^h\ 15^m, +45^\circ)$ (Ursa Major/Lynx) in the northern hemisphere (TA 2018)

The data used in the present work

The same as we used for UHECR18, 8–12 October 2018, Paris, France

- Energy thresholds chosen to match the measured integral fluxes in $-12° \leq \delta \leq +42°$
  - Mismatches of nominal energies within systematic uncertainties ($\pm 14\%_{\text{Auger}} \pm 21\%_{\text{TA}}$)
- **Lower-energy dataset** $\geq$ 8.86 EeV / $\geq$ 10 EeV
- **Higher-energy dataset** $\geq$ 40 EeV / $\geq$ 53.2 EeV

Auger data $E_{\text{Auger}} \geq 8.86$ EeV

- 01 Jan 2004 – 31 Aug 2016
- $\theta < 80°$[1] ($\delta < +44.8°$)
- 78 400 km^2 yr sr (27k events)

TA data $E_{\text{TA}} \geq 10$ EeV

- 11 May 2018 – 10 May 2017
- $\theta < 55°$ ($\delta > -15.7°$)
- 11 500 km^2 yr sr (4k events)

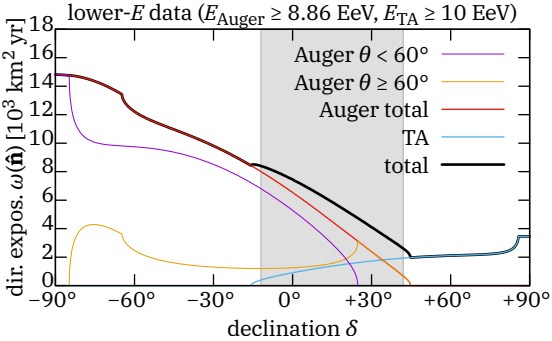

[1] Different quality cuts and reconstruction techniques for $\theta \lessgtr 60°$

The data used in the present work

The same as we used for UHECR18, 8–12 October 2018, Paris, France

- Energy thresholds chosen to match the measured integral fluxes in $-12° \leq \delta \leq +42°$
  - Mismatches of nominal energies within systematic uncertainties ($\pm 14\%_{\text{Auger}} \pm 21\%_{\text{TA}}$)
- **Lower-energy dataset** $\geq$ 8.86 EeV / $\geq$ 10 EeV
- **Higher-energy dataset** $\geq$ 40 EeV / $\geq$ 53.2 EeV

Auger data $E_{\text{Auger}} \geq 40$ EeV

- 01 Jan 2004 – **30 Apr 2017**
- $\theta < 80°$[1] ($\delta < +44.8°$)
- 91 300 km^2 yr sr (842 events)

TA data $E_{\text{TA}} \geq 53.2$ EeV

- 11 May 2018 – 10 May 2017
- $\theta < 55°$ ($\delta > -15.7°$)
- 11 600 km^2 yr sr (127 events)

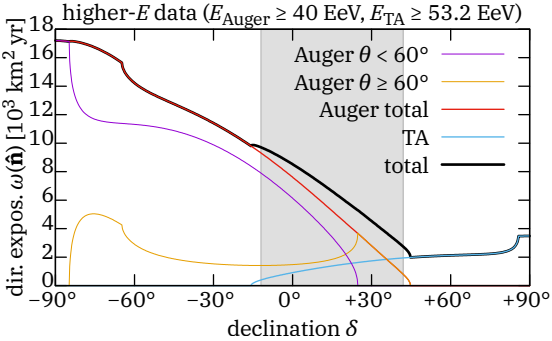

[1] Different quality cuts and reconstruction techniques for $\theta \lessgtr 60°$

Search for full-sky large-scale anisotropies at relatively low energies

Analysis unbiased regardless of higher multipoles (only possible with full-sky coverage, see UHECR18 for details)

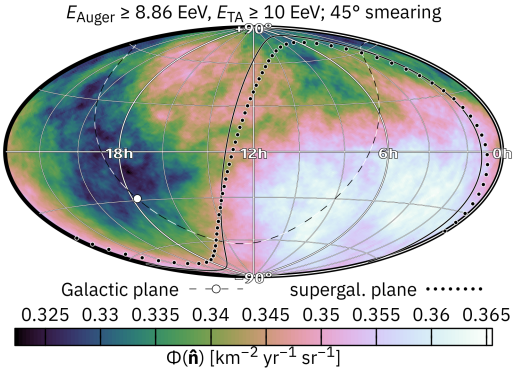

- Indication for a dipole moment:

$$d_x = (-0.7 \pm 1.1_{\text{stat}} \pm 0.01_{\text{calib}})\%$$
$$d_y = (+4.2 \pm 1.1_{\text{stat}} \pm 0.04_{\text{calib}})\%$$
$$d_z = (-2.6 \pm 1.3_{\text{stat}} \pm 1.4_{\text{calib}})\% \ (\pm 1.9\%_{\text{tot}})$$

  - For comparison, Auger 2018 ($E \geq 8$ EeV):

$\ell_{\max} = 1$	$\ell_{\max} = 2$
$d_x = (-1.0 \pm 1.0)\%$	$d_x = (-0.3 \pm 1.3)\%$
$d_y = (+5.9 \pm 1.0)\%$	$d_y = (+5.0 \pm 1.3)\%$
$d_z = (-2.6 \pm 1.5)\%$	$d_z = (-2 \quad \pm 4)\%$

  - Angular power spectrum coefficient:
    - $10^3 C_1 = 3.5$ ($p = 1.3\%$)
    - Expected: 0.8 ± 0.8; 99th perc.: 3.8

- Search for a quadrupole moment:
  - Angular power spectrum coefficient: $10^3 C_2 = 1.3$ ($p = 5.5\%$)
  - Expected from fluct. (assuming isotropy): mean $\pm$ st.dev. $= 0.6 \pm 0.4$ (99th percentile $= 1.9$) (including uncertainty in energy cross-calibration)

Blind search for medium-scale anisotropies at the highest energies

Scan over circular windows with 7 radii ($5°, 10°, \ldots, 35°$), 49 152 centers ($\approx 0.9°$ HEALPix grid)

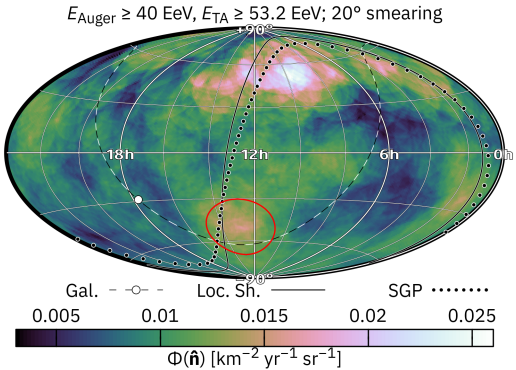

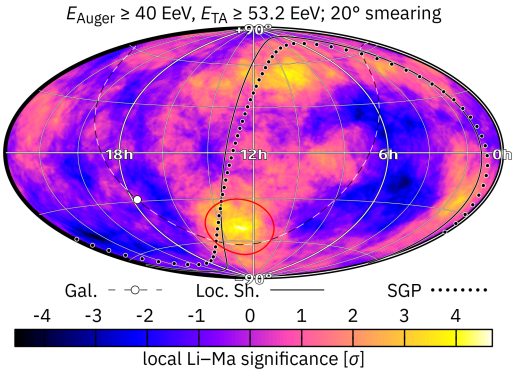

Most statistically significant excesses:

- **20°** radius around ($12^{\text{h}}\ 50^{\text{m}}, -50°$) 4.7σ pre-trial (2.2σ post-trial)
- 15° radius around ($9^{\text{h}}\ 30^{\text{m}}, +54°$) 4.2σ pre-trial (1.5σ post-trial)

Blind search for medium-scale anisotropies at the highest energies

Scan over circular windows with 7 radii (5°, 10°, . . . , 35°), 49 152 centers (≈ 0.9° HEALPix grid)

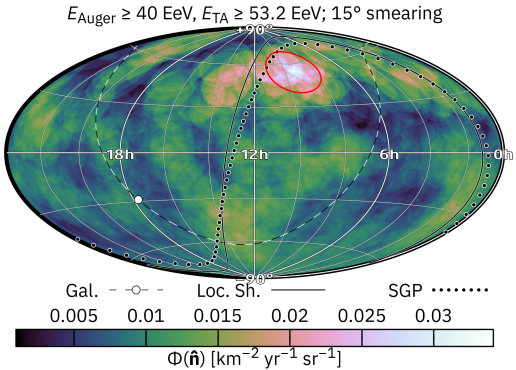

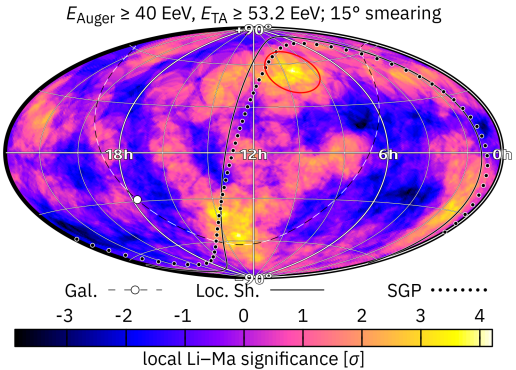

Most statistically significant excesses:

- 20° radius around ($12^{\text{h}}\ 50^{\text{m}}, -50°$) 4.7$\sigma$ pre-trial (2.2σ post-trial)
- **15°** radius around ($9^{\text{h}}\ 30^{\text{m}}, +54°$) 4.2$\sigma$ pre-trial (1.5σ post-trial)

The supergalactic plane and the Local Sheet

Supergalactic plane

- Defined in 1953 by Gérard de Vaucouleurs
- Based on the distribution of matter on several tens of Mpc scale
- Very well known and widely used for decades
- Tilted by 74° w.r.t. celestial equator, 84° w.r.t. Galactic plane

Local Sheet →

- Includes nearly all galaxies $\lesssim$ 6 Mpc from us (M. L. McCall 2014)
- Mostly consists of 12 large galaxies in a ring ("Council of Giants") and 2 more in the middle (Milky Way and M31) plus their satellites
- Tilted by 81° w.r.t. equator, 89° w.r.t. Gal. plane, 8° w.r.t. SGP

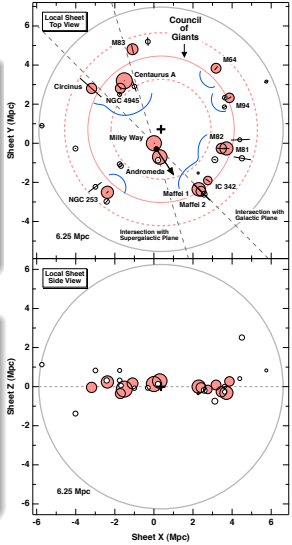

The analysis

For a given angular size X:

- **"On" region**: $\pm X$ band around SGP or Local Sheet
- **"Off" region**: rest of the sky
- Integrated **exposures**: $\mathcal{E}_{\rm on}$, $\mathcal{E}_{\rm off}$, $\mathcal{E}_{\rm tot} = \mathcal{E}_{\rm on} + \mathcal{E}_{\rm off} \approx 103\,000$ km^2 yr sr
- **Numbers of events**: $N_{\rm on}$, $N_{\rm off}$, $N_{\rm tot} = N_{\rm on} + N_{\rm off} = 969$
- Local **Li–Ma significance**: $\pm\sqrt{-2\left(N_{\rm on}\ln N_{\rm on}/\mathcal{E}_{\rm on} + N_{\rm off}\ln N_{\rm off}/\mathcal{E}_{\rm off} - N_{\rm tot}\ln N_{\rm tot}/\mathcal{E}_{\rm tot}\right)}$
  (+ if $N_{\rm on}/\mathcal{E}_{\rm on} > N_{\rm off}/\mathcal{E}_{\rm off}$, − otherwise)
  - Term in round parentheses: log-likelihood ratio between null hypothesis and best alternative
  - $\approx$ Gaussian$(\mu = 0, \sigma = 1)$ if $N_{\rm on}, N_{\rm off} \gg 1$ and the null hypothesis (isotropic flux) is true

- Repeat for $X = 5°, 6°, \ldots, 35°$ and pick the highest local significance.
- Do the same with millions of Monte Carlo datasets generated assuming an isotropic flux ($N_{\rm on} \propto \mathcal{E}_{\rm on} \pm$ binomial fluctuations) in order to compute the post-trial significance.

Results

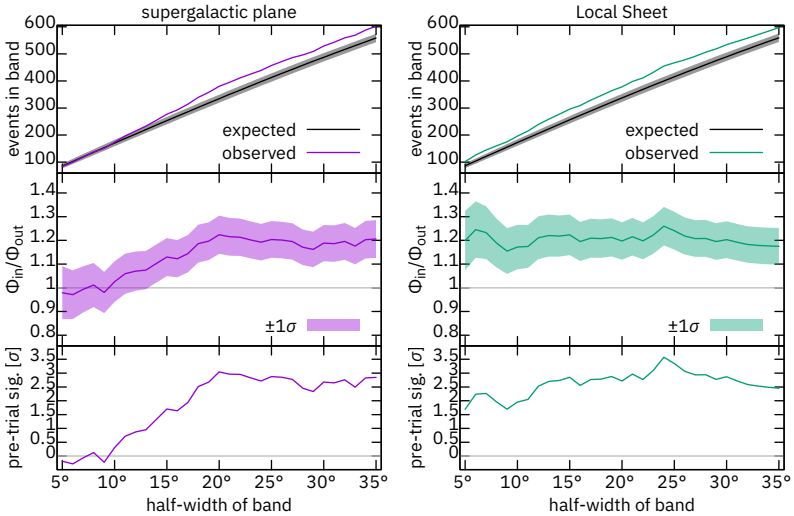

Best significance

- 3.6σ in $\pm 24°$ band around Local Sheet
- 455 events observed, 400 ± 15 expected[1]

Best significance around supergalactic plane

- 3.0σ in $\pm 20°$ band
- 380 events observed, 335 ± 15 expected[1]

[1] binom. with $n = 969, p = \mathscr{E}_{on}/\mathscr{E}_{tot}$

Discussion

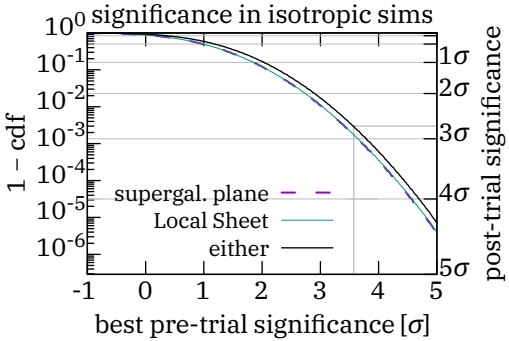

(Effects of cross-calib. uncertainty found negligible here)

- Post-trial significance taking into account multiple trials: 2.8σ ($p = 0.3\%$)
  - Penalty for using both planes < 2, because only 8° tilt → bands mostly overlap
  - If we had scanned over energy thresholds (as in Auger (2015) using **part** (62.1%) of the current dataset): post-trial $p \lesssim 2\%$ (but **no energy threshold scan was actually performed in this work**!)

Previous studies

- T. Stanev et al. (1995) using Haverah Park data: $p = 0.6\%$ via $\sqrt{\langle b_{\rm SG}^2 \rangle}$
- T. Stanev (arXiv) using Auger (2008) data: 3.6σ pre-trial in "updated SGP" $\pm 10°$
- Auger (2015): $p = 3.5\%$ pre-trial (SGP $\pm 19°$, ≥ 53 EeV), 22% post-trial
- TA (preliminary): higher $E_{\rm cut}$ inside SGP $\pm 30°$ than outside (3.2σ, no scan)

Summary and future directions

Current results

- "low" E: 5% dipole moment ($p = 1.3\%$, sizeable uncertainty due to energy calibration)
- "high" E: 26% higher flux within 24° of Local Sheet than elsewhere ($p = 0.3\%$ post-trial)

Possible new analyses

- Correlations with galaxy catalogs taking propagation effects into account
- Searches for large-scale anisotropies with more energy thresholds
  - AdM and P. Tinyakov (2018) predict best worst-case sensitivity at $E_{\min} \sim 30$ EeV

New detectors being deployed

AugerPrime → high-energy composition observable → high-rigidity (E/Z) samples

TA×4 → high-energy anisotropies in the northern hemisphere with more statistics

Stay tuned!

Back-up slides

Telescope Array 53.2 vs 57 EeV

- Coldspot below $10^{19.75}$ eV and hotspot above
- When lowering the energy threshold, the coldspot starts to cancel out the hotspot.

number of events	$E < 57$EeV	$E \geq 57$EeV	total	exposure
within 15° of ($9^h\ 30^m, +54°$)	0	16	16	3.8%
elsewhere	18	93	111	96.2%
total	18	109	127	100%
local Li–Ma significance	-1.2σ	$+4.6\sigma$	$+4.1\sigma$	

Search for full-sky large-scale anisotropies at relatively low energies

Analysis unbiased regardless of higher multipoles (only possible with full-sky coverage, see UHECR18 for details)

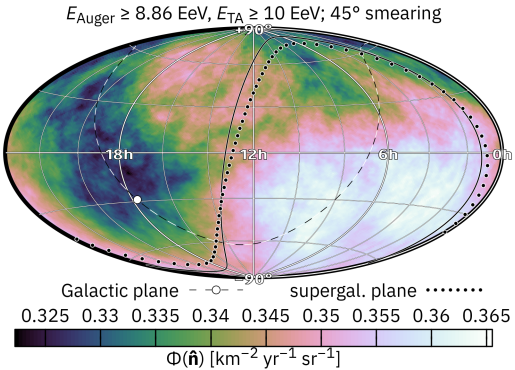

- Indication for a dipole moment:

$$d_x = (-0.7 \pm 1.1)\%$$
$$d_y = (+4.2 \pm 1.1)\%$$
$$d_z = (-2.6 \pm 1.9)\%$$

  - For comparison, Auger 2018 ($E \geq 8$ EeV):

$\ell_{\max} = 1$	$\ell_{\max} = 2$
$d_x = (-1.0 \pm 1.0)\%$	$d_x = (-0.3 \pm 1.3)\%$
$d_y = (+5.9 \pm 1.0)\%$	$d_y = (+5.0 \pm 1.3)\%$
$d_z = (-2.6 \pm 1.5)\%$	$d_z = (-2 \quad \pm 4)\%$

  - Angular power spectrum coefficient:
    - $10^3 C_1 = 3.5$ ($p = 1.3\%$)
    - Expected: 0.8 ± 0.8; 99th perc.: 3.8

- Search for a quadrupole moment:
  - Angular power spectrum coefficient: $10^3 C_2 = 1.32$ ($p = 5.5\%$)
  - Expected from fluct. (assuming isotropy): mean $\pm$ st.dev. $= 0.60 \pm 0.39$ (99th percent. $= 1.86$) (including uncertainty in energy cross-calibration)

Search for full-sky large-scale anisotropies at relatively low energies

Analysis unbiased regardless of higher multipoles (only possible with full-sky coverage, see UHECR18 for details)

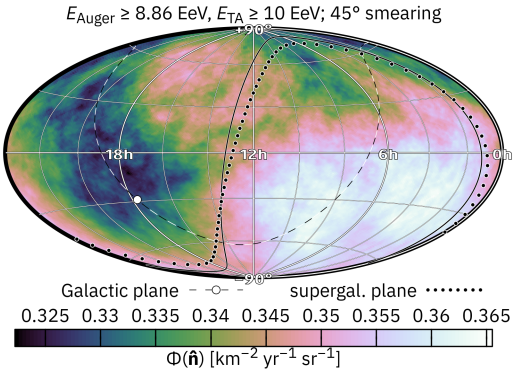

- Indication for a dipole moment:

$$d_x = (-0.7 \pm 1.1)\%$$
$$d_y = (+4.2 \pm 1.1)\%$$
$$d_z = (-2.6 \pm 1.3)\%$$

  - For comparison, Auger 2018 ($E \geq 8$ EeV):

$\ell_{\max} = 1$	$\ell_{\max} = 2$
$d_x = (-1.0 \pm 1.0)\%$	$d_x = (-0.3 \pm 1.3)\%$
$d_y = (+5.9 \pm 1.0)\%$	$d_y = (+5.0 \pm 1.3)\%$
$d_z = (-2.6 \pm 1.5)\%$	$d_z = (-2 \quad \pm 4)\%$

  - Angular power spectrum coefficient:
    - $10^3 C_1 = 3.5$ ($p = 0.05\%$)
    - Expected: 0.6 ± 0.5; 99th perc.: 2.2

- Search for a quadrupole moment:
  - Angular power spectrum coefficient: $10^3 C_2 = 1.32$ ($p = 4.2\%$)
  - Expected from fluct. (assuming isotropy): mean $\pm$ st.dev. $= 0.57 \pm 0.36$ (99th percent. $= 1.74$) (excluding uncertainty in energy cross-calibration)

$E_{\text{Auger}} \geq 8.86$ EeV, $E_{\text{TA}} \geq 10$ EeV; 45° smearing

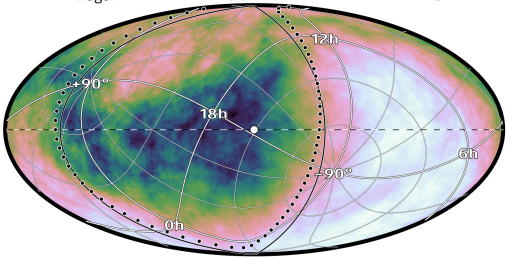

Galactic plane – –○– – supergal. plane ·····

0.325 0.33 0.335 0.34 0.345 0.35 0.355 0.36 0.365

$\Phi(\hat{\mathbf{n}})$ [km^{-2} yr^{-1} sr^{-1}]

$E_{\text{Auger}} \geq 8.86$ EeV, $E_{\text{TA}} \geq 10$ EeV; 45° smearing

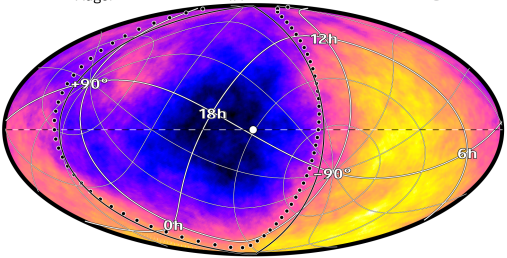

Galactic plane – –○– – supergal. plane ·····

-4 -2 0 2 4

local Li–Ma significance [σ]

$E_{\text{Auger}} \geq 8.86$ EeV, $E_{\text{TA}} \geq 10$ EeV; 45° smearing

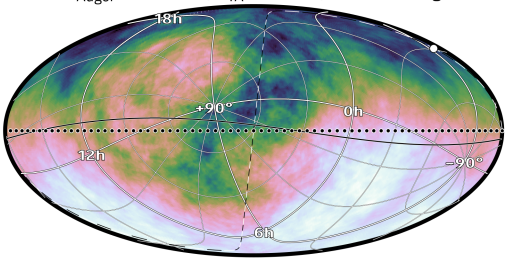

Galactic plane – –○– – supergal. plane ·····

$E_{\text{Auger}} \geq 8.86$ EeV, $E_{\text{TA}} \geq 10$ EeV; 45° smearing

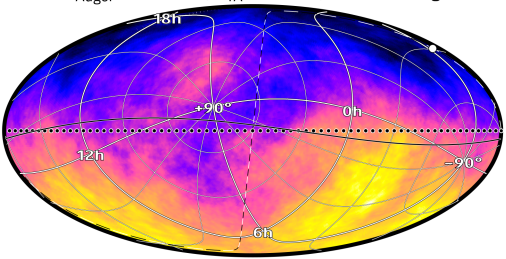

Galactic plane – –○– – supergal. plane ·····

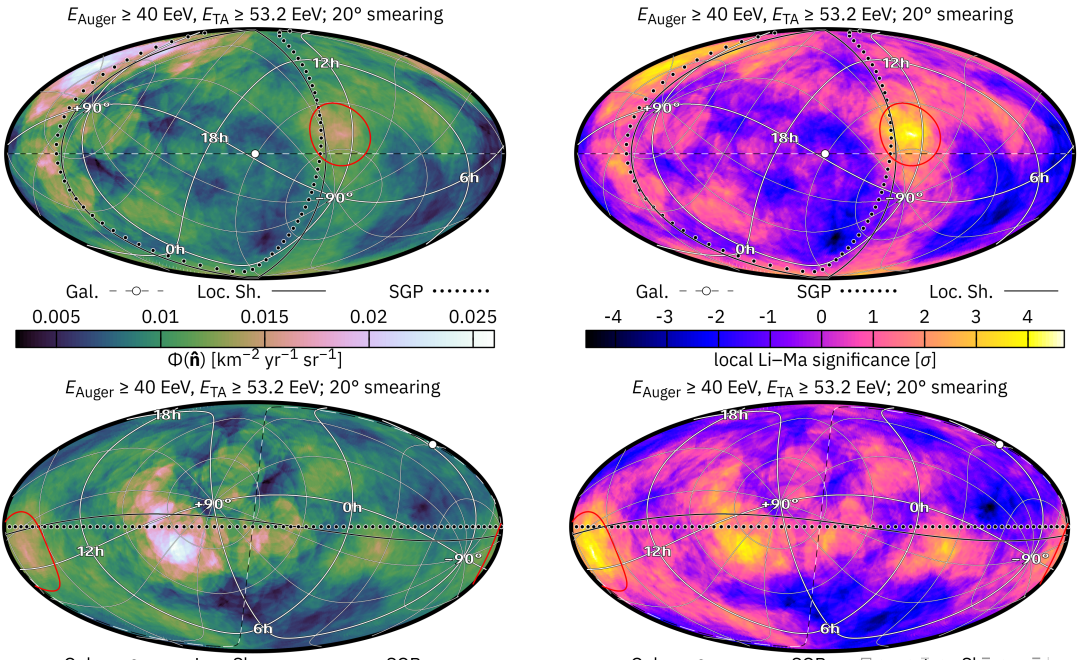
$E_{\text{Auger}} \geq 40$ EeV, $E_{\text{TA}} \geq 53.2$ EeV; 20° smearing
12h
+90°
18h
6h
−90°
0h
Gal.
Loc. Sh.
SGP
0.005
0.01
0.015
0.02
0.025
$\Phi(\hat{\mathbf{n}})$ [km^{-2} yr^{-1} sr^{-1}]
$E_{\text{Auger}} \geq 40$ EeV, $E_{\text{TA}} \geq 53.2$ EeV; 20° smearing
12h
+90°
18h
6h
−90°
0h
Gal.
SGP
Loc. Sh.
-4
-3
-2
-1
0
1
2
3
4
local Li–Ma significance [σ]
$E_{\text{Auger}} \geq 40$ EeV, $E_{\text{TA}} \geq 53.2$ EeV; 20° smearing
18h
+90°
0h
12h
−90°
6h
Gal.
Loc. Sh.
SGP
$E_{\text{Auger}} \geq 40$ EeV, $E_{\text{TA}} \geq 53.2$ EeV; 20° smearing
18h
+90°
0h
12h
−90°
6h
Gal.
SGP
Loc. Sh.

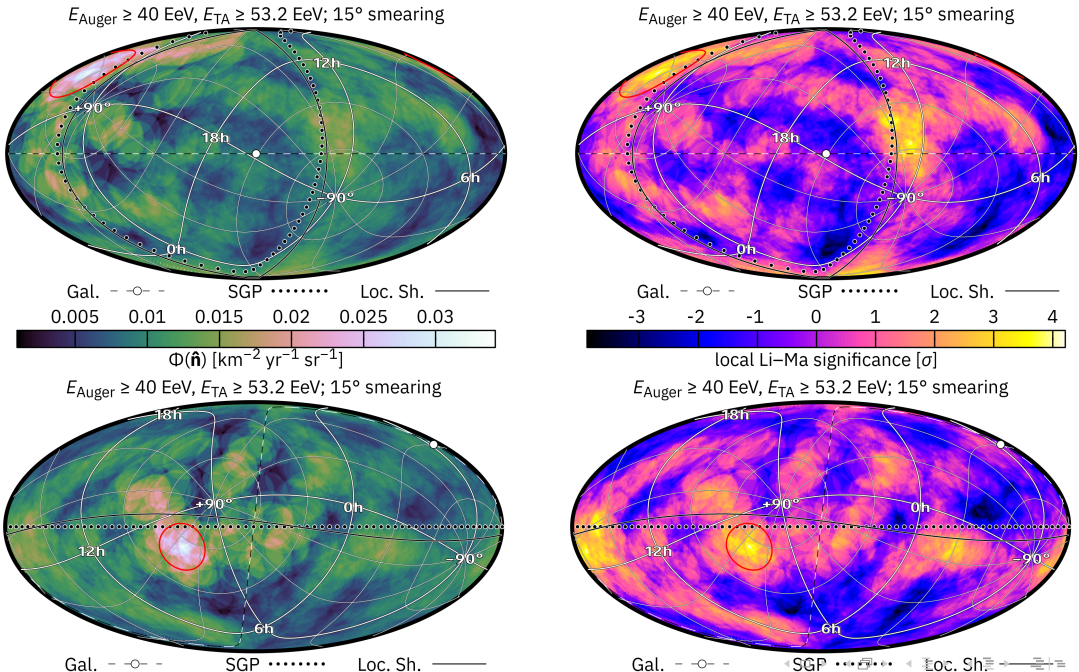
$E_{\text{Auger}} \geq 40$ EeV, $E_{\text{TA}} \geq 53.2$ EeV; 15° smearing
12h
+90°
18h
6h
−90°
0h
Gal.
SGP
Loc. Sh.
0.005
0.01
0.015
0.02
0.025
0.03
$\Phi(\hat{\mathbf{n}})$ [km^{-2} yr^{-1} sr^{-1}]
$E_{\text{Auger}} \geq 40$ EeV, $E_{\text{TA}} \geq 53.2$ EeV; 15° smearing
12h
+90°
18h
6h
−90°
0h
Gal.
SGP
Loc. Sh.
-3
-2
-1
0
1
2
3
4
local Li–Ma significance [σ]
$E_{\text{Auger}} \geq 40$ EeV, $E_{\text{TA}} \geq 53.2$ EeV; 15° smearing
18h
+90°
0h
12h
−90°
6h
Gal.
SGP
Loc. Sh.
$E_{\text{Auger}} \geq 40$ EeV, $E_{\text{TA}} \geq 53.2$ EeV; 15° smearing
18h
+90°
0h
12h
−90°
6h
Gal.
SGP
Loc. Sh.

TA×4 overview

E. Kido (this conference, CRI1b, Thu 25 Jul 14:00)
PoS(ICRC2019)312

Summary

- Implications on anisotropy were obtained by the TA experiment.
- Arrangement of TAx4 detectors:
  - **500 new** SDs with **2.08 km** spacing + TA SDs
    → Coverage of **4**× TA SDs ～3000 km^2
  - **2 new** Fluorescence Detector (FD) stations (4+8 HiRes Telescopes)
- More than half of TAx4 SDs were deployed.
- North TAx4 FD was constructed.
- Data acquisition was started.

  SD: from Apr. 2019, FD: from Jun. 2018
- Cosmic ray events are being collected.
- Prospects
  - Hotspot and spectrum anisotropy with E > 57 EeV will be studied with ～**4**× TA SD equivalent statistics if the full operation is started.
  - Xmax: ～**3**× TA SDFD equivalent events will be expected at the highest energies if the full operation is started.

19